

1 **CLASSIFICATION.** Major category: Biological Sciences. Minor category: Microbiology.

2 **The non-contiguous operon: a novel genetic organization to coordinate bacterial**
3 **gene expression**

4

5 S. Saenz-Lahoya^a, N. Bitarte^a, B. García^a, S. Burgui^a, M. Vergara-Irigaray^a, J. Valle^a, C.
6 Solano^a, A. Toledo-Arana^b and I. Lasa^{a*}

7 ^a Laboratory of Microbial Pathogenesis. Navarrabiomed, Complejo Hospitalario de
8 Navarra (CHN)-Universidad Pública de Navarra (UPNA), IDISNA, Pamplona-
9 31008, Spain

10 ^b Instituto de Agrobiotecnología. IDAB, CSIC-UPNA-Gobierno de Navarra. 31192-
11 Mutilva, Navarra, Spain.

12

13 * Corresponding author: Iñigo Lasa.

14 To whom correspondence should be addressed: Iñigo Lasa. Laboratory of Microbial
15 Pathogenesis. Navarrabiomed-Complejo Hospitalario de Navarra (CHN)-Universidad
16 Pública de Navarra (UPNA), IDISNA, Pamplona-31008, Spain

17 E-mail: ilasa@unavarra.es

18

19 **Keywords:** operon, antisense transcription, overlapping transcription, *Staphylococcus*
20 *aureus*, RNase III, menaquinone.

21

22

23 **ABSTRACT**

24 Bacterial genes are typically grouped into operons defined as clusters of adjacent
25 genes encoding for proteins that fill related roles and are transcribed into a single
26 polycistronic mRNA molecule. This simple organization provides an efficient
27 mechanism to coordinate the expression of neighboring genes and is at the basis of
28 gene regulation in bacteria. Here, we report the existence of a higher level of
29 organization in operon structure that we named non-contiguous operon and consists in
30 an operon containing a gene (s) that is transcribed in the opposite direction to the rest
31 of the operon. This novel transcriptional architecture is exemplified by the genes *menE-*
32 *menC-MW1733-ytkD-MW1731* involved in menaquinone synthesis in the major human
33 pathogen *Staphylococcus aureus*. We show that *menE-menC-ytkD-MW1731* genes
34 are transcribed as a single transcription unit whereas the *MW1733* gene, located
35 between *menC* and *ytkD*, is transcribed in the opposite direction. This
36 genomic organization generates overlapping transcripts whose expression is mutually
37 regulated by transcriptional interference and RNase III processing at the overlapping
38 region. In the light of our results, the canonical view of operon structure should be
39 revisited by including this novel operon arrangement in which co-transcription and
40 overlapping transcription are combined to coordinate functionally related gene
41 expression.

42

43 **Significance**

44 In bacteria, functionally related genes are often co-transcribed in a single mRNA
45 molecule under the same upstream promoter, forming a polycistronic operon unit. With
46 this strategy, bacteria guarantee that production of all proteins related to a specific
47 cellular process is simultaneously switched on or off. Here, we report the identification
48 of a novel transcriptional organization consisting in operons that contain a gene(s) that
49 is transcribed in the opposite direction to the rest of the genes of the operon. As a
50 consequence, the resulting mRNA is fully complementary to the operon transcript. This
51 genetic arrangement leads to mutual regulation of the overlapping transcripts
52 expression and thus provides an additional strategy for coordinating the expression of
53 functionally related genes within an operon.

54 \body

55 **INTRODUCTION**

56 The term operon was first proposed by F. Jacob and J. Monod as a functional genomic
57 DNA unit containing a group of genes that are transcribed together under the control of
58 a single promoter (1). This concept served to explain a revolutionary model of bacterial
59 gene regulation, in which expression of a cluster of genes was negatively controlled by
60 a repressor acting at a single operator that coordinated the process. Over time, it has
61 been shown that operon gene regulation is much more complex than originally
62 expected, with operons that can be positively and/or negatively regulated at different
63 levels other than transcription initiation (2-4). The overall simplicity of operon
64 organization for coordinating gene expression explains why a substantial fraction of
65 functionally related bacterial genes are organized into operons (5, 6).

66 The list of operons in a specific genome can be predicted with reasonable accuracy
67 based on features such as the distance between each adjacent gene, the likelihood of
68 a pair of genes to be neighbors in a group of reference genomes and the phylogenetic
69 distance (7-9). However, these features are predisposed by the classical operon
70 concept and consequently, the identification of variations in genetic organization inside
71 operon structure through bioinformatic predictions has been very limited. The
72 development of RNA deep sequencing technologies is helping to elucidate 'operons' in
73 their full complexities by precisely defining the beginning and the end of mRNA
74 molecules and revealing the changes in the structure of statically predicted operons
75 under different experimental conditions (4, 10-17). An unexpected finding unraveled by
76 the precise determination of transcript boundaries is that very often convergent
77 operons overlap at their 3' end (tail to tail) and divergent operons overlap at their 5' end
78 (head to head). In these situations, the mRNA contributes to the expression of operon
79 genes, and at the same time, a region of the mRNA acts as an antisense transcript,
80 affecting the expression of the contiguous operon. The simultaneous sense and
81 antisense functions for transcript boundaries were reported under the term excludon in

82 *Listeria monocytogenes* (18). This genomic organization allows the establishment of a
83 regulatory relationship that results in the “exclusive” expression of only one of both
84 coding regions. The mechanisms for exclusion mediated regulation is multifaceted and
85 it can include transcription interference, transcription attenuation, degradation of the
86 double-stranded overlapping RNAs or stabilization of the RNAs after cleavage (19, 20).
87 In a previous work, and through a genome wide transcriptome profiling of the pathogen
88 *Staphylococcus aureus* (21), we identified several examples of groups of genes that
89 were apparently transcribed together despite they were separated by gene(s)
90 transcribed in the opposite direction. This transcriptional organization is an extreme
91 example of an exclusion, since the mRNA encoded on the opposite strand of DNA to
92 the operon would serve as a canonical mRNA that encodes for a protein while acting
93 as an antisense RNA, base-pairing all along its length with an internal untranslated
94 region of the polycistronic mRNA. Here, we report the existence of this new
95 transcriptional organization in an operon involved in the synthesis of menaquinone in *S.*
96 *aureus*. Our results demonstrate that the expression of both overlapping transcripts is
97 mutually regulated by transcriptional interference and endoribonuclease mediated
98 digestion. The existence of this genetic arrangement that we named non-contiguous
99 operon, confirms overlapping transcription as a specific mechanism for regulating gene
100 expression within an operon. In addition, it underlines the relevance of reviewing
101 operon structures in bacterial genomes to identify all protein partners whose
102 expression is coordinated in a particular cellular process.
103

104 RESULTS

105 Identification of “non-contiguous operons” in the *S. aureus* genome

106 We screened genome-wide the transcriptome data obtained from the clinical isolates *S.*
107 *aureus* 15981 (21) and *S. aureus* MW2 to identify genes cotranscribed together despite
108 being separated by a gene transcribed in the opposite direction. We found six
109 examples that fit the predicted model (Fig. 1, S1 and S2). RNA sequencing data of
110 published results from different laboratories (<http://rnamaps.unavarra.es/>) confirmed
111 the existence of identical transcriptional organizations in five other genetically unrelated
112 *S. aureus* strains (Fig.1, S1 and S2). The function of most of the proteins encoded by
113 such operons is unknown. CoaD, which is part of the coenzyme A biosynthesis
114 pathway, MenADB and MenEC, required for menaquinone synthesis, and MoaABCED,
115 required for molybdate transport, are among the proteins with known functions.

116 To explore the significance of this transcriptional organization, we chose the region
117 comprising *menE*, *menC*, *MW1733*, *ytkD* and *MW1731* genes based on the size of the
118 transcripts and the relevance of menaquinone synthesis during *S. aureus* infections
119 (22) (Fig. 1). *menE-menC* and *ytkD-MW1731* are listed as two independent operons in
120 the prokaryotic operons database (<http://csbl.bmb.uga.edu/DOOR/>) (23). However,
121 transcriptome data indicated that both operons are transcribed as a single
122 transcriptional unit (Fig. 1). These results agreed with published results obtained by
123 mapping of transcriptional start sites (TSS) by differential RNA-seq that revealed a
124 unique TSS upstream the *menE* gene (24) (Fig. 1). To experimentally confirm the
125 transcriptome results and because the environmental conditions controlling the
126 expression of *menE* remain unknown, we first generated two derivatives of the wild
127 type strain in which the promoter region upstream the *menE* gene was deleted (ΔP_{men}
128 strain) or replaced by the constitutive *blaZ* promoter (*P_{blaZ}-men* strain) (Fig. S3). For
129 each of these strains, we generated derivatives in which the chromosomal copy of
130 either *menC* or *MW1731* genes was tagged with the 3xFLAG sequence (Fig. S3) and
131 then examined MenC and MW1731 protein levels by western blotting. Consistent with

132 the transcriptome results, the $\Delta Pmen$ mutation correlated with inhibition of both MenC
133 and MW1731 proteins expression. Note that the $\Delta Pmen$ deletion did not completely
134 abolish protein production. On the contrary, the strains containing the constitutive BlaZ
135 promoter produced considerably higher levels of MenC and MW1731 compared with
136 the wild type strain (Fig. 2A). Thus, these findings suggested that expression of *ytkD*-
137 *MW1731* depends on the promoter region upstream the *menE* gene.

138 To further validate the cotranscription of *menE-menC-ytkD-MW1731* genes, we
139 performed northern-blot analysis using strand-specific riboprobes corresponding to
140 *menE-menC* (probe A) and *ytkD-MW1731* (probe B) coding regions with total RNA
141 from exponentially growing cells of the wild type strain, and its two isogenic derivatives,
142 $\Delta Pmen$ and *PblaZ-men*. Results showed that the mRNA expression levels are very low
143 in the wild type strain, because neither probe was able to detect the mRNA (Fig. 2B). In
144 contrast, both probe A and B hybridizations with *PblaZ-men* RNA revealed an
145 increased accumulation of a fuzzy band of approximately 4 kb that was compatible with
146 cotranscription of *menE-menC* with the downstream genes *ytkD-MW1731* (Fig. 2B).
147 Note that probe B also clearly detects an additional processing band (\approx 1.2kb).
148 Together, these results strongly suggest that *menE-menC* and *ytkD-MW1731*
149 expression depends on the promoter located upstream *menE*, which is consistent with
150 transcriptome data indicating that *menE-menC-ytkD-MW1731* genes comprise a single
151 transcriptional unit.

152 Transcriptome data also indicated that the *MW1733* gene (258 bp long) is transcribed
153 at high levels with a short 5' UTR of 26 nucleotides and a 3' UTR of 60 nucleotides that
154 overlaps the 3' end of the *menC* coding sequence. To confirm transcriptome data, we
155 generated two additional strains in which 27 nucleotides of the promoter region
156 upstream the *MW1733* gene were deleted ($\Delta PMW1733$ strain) or replaced by the
157 constitutive *blaZ* promoter (*PblaZ-MW1733* strain) (Fig. S3). For each of these strains,
158 we generated a derivative in which the chromosomal copy of the *MW1733* gene was

159 tagged with the 3xFLAG sequence (Fig. S3). As expected, analysis of MW1733 protein
160 levels revealed that $\Delta PMW1733$ mutation correlated with inhibition of MW1733 protein
161 production whereas transcription from the constitutive *BlaZ* promoter led to higher
162 levels of MW1733 compared with those in the wild type strain (Fig. 2A). Finally, we
163 performed a northern-blot analysis using a strand-specific riboprobe corresponding to
164 the *MW1733* coding region (probe C) with total RNA from exponentially growing cells of
165 the wild type, $\Delta PMW1733$ and *PblaZ-MW1733* strains. Results showed the presence of
166 a discrete band of approximately 350 nucleotides in the wild type strain (Fig. 2B).
167 Hybridization with $\Delta PMW1733$ and *PblaZ-MW1733* RNA revealed a decreased and
168 increased accumulation of the RNA product, respectively.
169 Overall, these results describe an operon organization which is novel in the sense that
170 all the genes of the operon are not contiguous and therefore, we refer to it as “non-
171 contiguous operon”. The first two genes are followed by a gene transcribed from the
172 opposite strand, this gene is then followed by two other genes cotranscribed with the
173 first two. In this spatial transcriptional organization, the non-coding region of the
174 tetracistronic transcript completely overlaps the monocistronic unit.

175

176 ***The expression of the menE-menC-ytkD-MW1731 operon and the MW1733 gene***
177 **is reciprocally regulated**

178 To determine whether transcriptional levels of *menE-menC-ytkD-MW1731* have an
179 effect on the amount of *MW1733* mRNA, we compared by northern blot the transcript
180 levels of *MW1733* in the wild type, $\Delta Pmen$ and *PblaZ-men* strains using probe C to
181 detect *MW1733* mRNA. Results showed that *MW1733* transcript levels slightly
182 increased when transcription of the operon was inhibited and on the other hand,
183 markedly decreased in *PblaZ-men* strain, that is under the presence of an excess of
184 the overlapping tetracistronic transcript (Fig. 3A). To confirm the regulation of *MW1733*
185 expression at a protein level, we constructed derivatives of $\Delta Pmen$ and *PblaZ-men*

186 containing the chromosomal copy of the *MW1733* gene tagged with a 3xFLAG epitope
187 at the C-terminus (Fig. S4). Consistent with northern-blot results, *MW1733* protein
188 levels significantly decreased in *PblaZ-men* compared to those in the wild type strain
189 (Fig. 3A).

190 Next, we investigated the possibility of a reciprocal effect of *MW1733* mRNA levels on
191 the expression of the tetracistronic operon. To do so, we firstly analysed by northern
192 blot, and with the use of probe A, *menE-menC-ytkD-MW1731* mRNA levels in the wild
193 type, $\Delta PMW1733$ and *PblaZ-MW1733* strains. In agreement with the low level of
194 expression of the tetracistronic mRNA in the wild type strain (Fig. 2B), we could not find
195 a significant difference in *menE-menC-ytkD-MW1731* mRNA levels between strains
196 when probe A was used (Fig. 3B). Thus, we repeated the northern blot assay with the
197 use of probe B, specific for *ytkD-MW1731*. Again, the *ytkD-MW1731* transcript was
198 undetectable in the wild type and $\Delta PMW1733$ strains. However, when *MW1733* was
199 overexpressed, a specific processing transcript was detected. The size of the discrete
200 band (≈ 1.5 kb) is consistent with a transcript including *ytkD-MW1731* that might be
201 obtained upon processing of the *menE-menC-ytkD-MW1731* mRNA (Fig. 3C). Next, we
202 constructed derivatives of $\Delta PMW1733$ and *PblaZ-MW1733* harbouring a chromosomal
203 copy of either *menC* or *MW1731* tagged with the 3xFLAG epitope in the carboxy-
204 terminal domain (Fig. S4). Notably, constitutive expression of *MW1733* caused a clear
205 reduction in the levels of the MenC protein (Fig. 3B) and a significant accumulation of
206 *MW1731* protein levels in *PblaZ-MW1733* compared to the wild type strain (Fig. 3C).

207 Collectively, these results support the notion that in the non-contiguous operon,
208 transcriptional units generated from opposite strands regulate each other's expression.
209 Thus, in the non-contiguous operon under study, an increase in tetracistronic operon
210 transcription negatively regulates the expression of the interspersed *MW1733* gene.
211 Reciprocally, an increase in *MW1733* mRNA discoordinates expression within the

212 overlapped operon, by strongly elevating *ytkD-MW1731* mRNA levels while reducing
213 *menE-menC* expression.

214

215 **Analysis of the mechanisms underlying the regulation of non-contiguous** 216 **operons expression**

217 RNase III endoribonuclease is responsible for processing overlapping sense/antisense
218 transcripts genome wide in bacteria (21, 25, 26). Thus, we examined the importance of
219 RNase III activity in the reduction of *MW1733* transcript levels when an excess of
220 *menE-menC-ytkD-MW1731* is transcribed. Deletion of RNase III both in the wild type
221 strain and in the strain overproducing the tetracistronic operon (*PblaZ-men*) (Fig. S5),
222 caused a slight increase in the amount of *MW1733* mRNA (Fig. 4A). Consequently,
223 *MW1733* protein levels only moderately increased in *rnc* mutants compared to those in
224 the respective RNase III producing strains (Fig. 4A). On the other hand, we studied the
225 involvement of RNase III in *menE-menC-ytkD-MW1731* mRNA processing when
226 *MW1733* is overexpressed. A northern blot, using probe A, with RNA from cells of the
227 wild type, *PblaZ-MW1733*, and their corresponding *rnc* mutants showed no significant
228 differences between strains, given the low detectability of *menE-menC-ytkD-MW1731*
229 mRNA (Fig. 4B). Secondly, we carried out a similar northern blot, but with the use of
230 probe B, specific to detect *ytkD-MW1731* mRNA. Results revealed that processing of
231 the tetracistronic mRNA when an excess of *MW1733* is transcribed still occurred in the
232 absence of RNase III. However, in this case, the processing pattern of the operon
233 changed, leading to a significant decrease in the amount of the discrete 1.5 kb
234 transcript and to the appearance of two additional larger mRNA fragments (Fig. 4C).
235 Accordingly, *MW1731* protein levels decreased in *rnc* mutants of the wild type and
236 *PblaZ-MW1733* strains when compared to those in their respective RNase III producing
237 strains (Fig. 4C and Fig. S5). Overall, these results indicated that RNase III explains,
238 only to a certain extent, the *MW1733* mediated cleavage of *menE-menC-ytkD-MW1731*

239 mRNA, suggesting that additional ribonuclease(s) might also be responsible for this
240 processing.

241 Besides processing by RNase III, another possible explanation for the reciprocal
242 regulation of overlapping transcripts described above might be transcriptional
243 interference (27), defined as the suppressive influence that the convergent RNA
244 synthesis machinery from one DNA strand causes in *cis* on the transcription of the
245 neighboring gene. Thus, we next sought to determine whether the observed antisense
246 regulation of *menE-menC-ytkD-MW1731* over *MW1733* occurred when the *MW1733*
247 gene was expressed in another location of the chromosome. To do so, we inserted a
248 3xFLAG tagged *MW1733* gene under its own promoter next to the innocuous *attB* site
249 of the lipase gene in both $\Delta PMW1733$ and $\Delta PMW1733 PblaZ-men$ genetic
250 backgrounds (Fig. S6). Importantly, and contrary to what happens when *MW1733* is
251 located in its natural location, northern blot analysis of *MW1733* transcript levels
252 showed that these were only slightly reduced in the presence of an excess of *menE-*
253 *menC-ytkD-MW1731* mRNA when the *MW1733* gene was placed and expressed *in*
254 *trans* (Fig. 4D). Note that there is a marked difference in the size and abundance of
255 *MW1733* mRNA when it is ectopically expressed from the *attB* chromosomal location.
256 Consistent with northern blot results, western blot analysis showed that *MW1733*
257 protein levels were unaffected in the $\Delta PMW1733 PblaZ-men MW1733 trans$ strain
258 compared with those in the wild type strain (Fig. 4D). These results indicated that
259 *menE-menC-ytkD-MW1731* mediated suppressive influence on *MW1733* expression
260 requires *cis* localization of both transcripts. Lastly, to reinforce these results, we
261 overexpressed a 3xFLAG tagged *MW1733* gene ectopically from a plasmid in the wild
262 type strain harboring a chromosomal copy of either *menC* or *MW1731* tagged with the
263 3xFLAG epitope (Fig. S6) and analyzed MenC and *MW1731* levels by western blot.
264 Overexpression of *MW1733 in trans* did not have any impact on MenC or *MW1731*
265 production, showing that *MW1733* effect in discoordinating *menE-menC-YtkD-MW1731*
266 operon expression also requires *cis* localization of both transcripts (Fig. 4E). Overall,

267 the above results indicate the existence of a transcriptional interference mechanism of
268 gene regulation between the machinery that synthesizes the non-contiguous operon
269 mRNA and the one synthesizing the mRNA of the interspersed gene.

270

282 **High transcriptional levels of the *MW1733* gene can lead to the appearance of** 283 **SCVs**

284 The experiments shown above demonstrated that overexpression of *MW1733* mRNA
285 leads to reduced MenC protein levels (Fig. 3B). In *S. aureus*, the inhibition of the
286 synthesis of menaquinone has been associated with a slowed growth phenotype,
287 known as small colony variants (SCVs) (28). SCVs are frequently isolated from clinical
288 samples obtained from patients experiencing chronic infections by *S. aureus*. We
289 observed that the $\Delta Pmen$ strain constructed in this work, which still shows some
290 residual production of the MenC protein (Fig. 2A), produces colonies whose size are
291 smaller than the ones corresponding to the wild type strain though they are not as
292 small as the SCVs generated by deletion of *menE-menC* genes ($\Delta menEC$) (Fig. S7A).
293 Therefore, we wondered whether constitutive expression of *MW1733* might be followed
294 by the appearance of SCVs phenotypic hallmarks. To test this hypothesis, the promoter
295 of *MW1733* was replaced by the constitutive BlaZ promoter in $\Delta Pmen$ strain (Fig. S8).
296 The resulting strain produced colonies significantly smaller than the $\Delta Pmen$ strain and
297 exhibited several characteristics associated to *S. aureus* SCVs such as decreased
298 pigmentation and increased resistance to aminoglycosides (tobramycin, streptomycin,
299 gentamycin, and amikacin) than the wild-type strain (29) (Fig. S7B and C). These
300 results suggest that overexpression of *MW1733* suppresses the expression of its
301 convergent *menE-menC* genes, which in turn leads to suppressed menaquinone
302 synthesis and the appearance of a SCV phenotype.

303 To confirm that appearance of SCVs by *MW1733* overexpression in $\Delta Pmen$ strain
304 exclusively happened when *MW1733* and *menE-menC-YtkD-MW1731* mRNAs were

305 expressed *in cis*, we overexpressed the *MW1733* gene ectopically from a plasmid in
306 $\Delta Pmen$ strain and analyzed colony size on TSA plates. The resulting strain, $\Delta Pmen$
307 pCN40::*MW1733* (Fig. S7A and Fig. S8), showed the same phenotype as the $\Delta Pmen$
308 strain. Thus, we conclude that this non-contiguous operon transcriptional organization
309 constitutes an effective mechanism for regulating gene expression and ultimately for
310 controlling cell growth.

311

312 **DISCUSSION**

313 The novelty introduced by the “non-contiguous operon” concept is that genes within an
314 operon can be interspersed with genes divergently transcribed and that, consequently,
315 they do not necessarily need to be contiguous in the genome. This transcriptional
316 arrangement does not fit within the classical operon paradigm, explaining why it has
317 passed previously unnoticed. It is important to note that in all the examples of non-
318 contiguous operons in the *S. aureus* genome, coding sequences of the operon never
319 overlap the coding region of the interspersed gene. Thus, it appears that the non-
320 contiguous operon transcriptional architecture may be a result of evolutionary pressure
321 to minimize genome size and provide an additional strategy for coupling the expression
322 of functionally related polypeptides. Our results provide evidence of two mechanisms
323 by which the non-contiguous operon arrangement can coordinate gene expression.
324 The first mechanism is related with the generation of double stranded templates
325 between complementary overlapping RNAs that can modify mRNA stability or
326 translation (30, 31). We showed that RNase III digestion of the mRNA duplexes is
327 partially responsible for both the repression of *MW1733* expression and also for the
328 cleavage of the tetracistronic mRNA into two independent transcripts. The resulting two
329 halves might be translated into proteins at a similar or different rate than before the
330 cleavage. Our results indicate that transcriptional induction of the *MW1733* gene leads
331 on one hand, to a reduction in MenE protein levels and on the other, to the stabilization
332 of the *ytkD-MW1731* half and thus, to the accumulation of higher levels of *MW1731*

333 protein compared to the wild type strain. Specific RNase III cleavage at intercistronic
334 regions with alternative outcomes for the resulting mRNAs has been previously
335 reported in *E. coli* (32). Opdyke *et al.* showed that binding of the *cis* non-coding RNA
336 *gadY* to the intercistronic region of *gadXW* mRNA resulted in RNase III cleavage and
337 monocistronic transcripts accumulation, probably due to increased stability of single
338 transcripts. Similarly, binding of a *cis*-encoded non-coding RNA to the *cII-O* mRNA of λ
339 phage has been shown to be responsible for an RNase III processing event that is
340 followed by degradation of the upstream *cII* fragment while the downstream *O* mRNA
341 remains stable. Because the sRNA partially overlaps the *cII* coding sequence at its 3'
342 end, it was concluded that degradation of the *cII* transcript is due to RNase III
343 processing occurring at that region (33). Regarding the mechanisms underlying the
344 stabilization process, it is possible that cleavage might alter the secondary structure of
345 the transcripts so that they are less susceptible to degradation. RNase III is not the only
346 endonuclease involved in *MW1733* dependent processing of the *menE-menC-ytkD-*
347 *MW1731* operon because discrete RNA fragments from the tetracistronic operon are
348 still detected in the absence of RNase III when *MW1733* is overexpressed. An
349 important direction for future studies will be to identify such additional
350 endoribonuclease(s).

351 The second mechanism that contributes to coordinating mRNA expression within the
352 non-contiguous operon is transcriptional interference. Because the distance between
353 promoters of the tetracistronic operon and the *MW1733* gene is longer than 200
354 nucleotides, the most obvious explanation for transcriptional interference is the collision
355 between the RNA synthesis machinery from one DNA strand with the transcription
356 machinery from the other strand (34, 35). A major finding consistent with the existence
357 of transcriptional interference is that tetracistronic operon overexpression did not cause
358 any effect on *MW1733* mRNA levels when this was expressed in *trans* from a separate
359 genomic location. Similarly, the expression of *menC* and *MW1731* was unaffected
360 when *MW1733* was overexpressed in *trans* from a plasmid. Pairing between

361 complementary transcripts can occur regardless of whether they are expressed in *cis*
362 or *trans*, and therefore, digestion of overlapping transcripts by RNase III and additional
363 endoribonucleases should take place when *MW1733* is produced in *trans*. Thus, we
364 currently do not understand why *MW1733* overexpression in *trans* does not affect
365 *menC* and *MW1731* expression. One possibility is that pairing and processing of the
366 overlapping transcripts is less efficient when both complementary transcripts are
367 produced from separate genomic locations.

368 What are the benefits of the non-contiguous operon organization compared to regular
369 operons? The exact functions of overlapping transcription are still a matter of debate
370 and several authors defend that overlapping transcription are mainly the product of
371 transcriptional noise, arising at spurious promoters throughout the genome (36). The
372 existence and maintenance of non-contiguous operon transcriptional architecture is a
373 strong evidence that overlapping transcription represents a specific strategy for gene
374 regulation. We can imagine a number of ways the non-contiguous operon may create
375 higher-level organizational features that are adaptive compared to a regular operon.
376 First, it enables a discoordinated expression within the genes of the operon upstream
377 and downstream the overlapping gene, diminishing gene expression noise and
378 ensuring a more precise stoichiometry. Second, it allows endoribonuclease-dependent
379 removal of transcripts that escape the regular transcription repression process. Third, it
380 allows downregulation (exclusion) of the overlapping gene expression by transcript-
381 independent transcriptional interference. Finally, it saves space and decreases the
382 genetic load associated with selecting for a regulatory given motif. All these theoretical
383 benefits require future studies to fully explore the fitness advantages that this
384 transcriptional organization provides to bacteria.

385 The *menE-menC-MW1733-YtkD-MW1731* genetic arrangement is conserved across
386 the *Staphylococcus* genus, a fact that suggests high functional relevance (Fig. S9). We
387 have found an example of the regulatory possibilities of this transcriptional
388 arrangement in the emergence of a Small-Colony Variant (SCVs) phenotype

389 associated to menaquinone synthesis deficiency in *S. aureus* (37). Many efforts have
390 been made to identify auxotrophic mutations that result in the appearance of SCVs (28,
391 38). However, when examining *S. aureus* clinical and tissue-cultured induced SCVs,
392 only around 20% can be assigned to a defined auxotrophy implying that other
393 pathways underlying SCVs formation probably exist (37). Here, we have seen that an
394 increase in the transcription of *MW1733* can account for the induction of SCVs under
395 low polycistronic operon transcription levels, without the need to generate a mutation.
396 The generation of SCVs through this mechanism has the advantage of producing
397 variants able to rapidly switch and revert to the fast-growing wild type phenotype at the
398 earliest opportunity to generate and infection, without the fitness costs associated with
399 the generation of mutations and revertant mutations. In this way, the formation and
400 stability of SCVs would be modulated by environmental conditions affecting
401 transcriptional levels of both the *menE-menC-ytkD-MW1731* operon and the *MW1733*
402 gene and also by factors affecting the binding between overlapping transcripts and the
403 RNase III processing rate. Further work is needed to identify environmental stimuli able
404 to trigger SCVs through this mechanism.

405 Overall, our results add a further degree of complexity to the initial model of operon
406 gene regulation described by F. Jacob and J. Monod and highlight the functional
407 relevance of overlapping transcription as a mechanism to coordinate the expression
408 levels of bacterial neighbouring genes.

409

410 **MATERIALS AND METHODS**

411 *S. aureus* strain 15981 was used as the genetic background for all genetic
412 manipulations. A summary of strains used is provided in Table S1. Mutant strains,
413 3xFLAG tagged strains, strains harbouring the *P_{BlaZ}* promoter instead of native
414 promoters and strains containing a 3xFLAG tagged *MW1733* gene under its own
415 promoter next to the *attB* site of the lipase gene were generated via allelic replacement
416 using the pMAD vector (39) as described previously (40). For inactivation of *mrc*
417 (RNaseIII encoding gene), the previously described pMAD $\Delta mrc::cat86$ plasmid (21)
418 was used. Detailed materials and methods are described in SI Materials and Methods.
419

420 **ACKNOWLEDGMENTS**

421 We thank Jose R. Penadés for critical reading of the paper. This work was supported
422 by the Spanish Ministry of Economy and Competitiveness grants BIO2014-53530-R
423 and BIO2017-83035-R (AEI/FEDER, EU). A.T-A is supported by the European
424 Research Council (ERC) under the European Union's Horizon 2020 research and
425 innovation programme (Grant Agreement No. 646869).

426

427 **REFERENCES**

428

- 429 1. Jacob F, Monod J (1961) Genetic regulatory mechanisms in the synthesis of
430 proteins. *Journal of Molecular Biology* 3:318–356.
- 431 2. Mattheakis LC, Nomura M (1988) Feedback regulation of the *spc* operon in
432 *Escherichia coli*: translational coupling and mRNA processing. *J Bacteriol*
433 170(10):4484–4492.
- 434 3. Lim HN, Lee Y, Hussein R (2011) Fundamental relationship between operon
435 organization and gene expression. *Proc Natl Acad Sci U S A* 108(26):10626–
436 10631.
- 437 4. Conway T, et al. (2014) Unprecedented high-resolution view of bacterial operon
438 architecture revealed by RNA sequencing. *mBio* 5(4):e01442–14.
- 439 5. Okuda S, et al. (2007) Characterization of relationships between transcriptional
440 units and operon structures in *Bacillus subtilis* and *Escherichia coli*. *BMC*
441 *Genomics* 8(1):48.
- 442 6. Rocha EPC (2008) The organization of the bacterial genome. *Annu Rev Genet*
443 42:211–233.
- 444 7. Zheng Y, Szustakowski JD, Fortnow L, Roberts RJ, Kasif S (2002)
445 Computational identification of operons in microbial genomes. *Genome Res*
446 12(8):1221–1230.
- 447 8. Mao X, et al. (2014) DOOR 2.0: presenting operons and their functions through
448 dynamic and integrated views. *Nucleic Acids Res* 42(Database issue):D654–9.
- 449 9. Perteua M, Ayanbule K, Smedinghoff M, Salzberg SL (2009) OperonDB: a
450 comprehensive database of predicted operons in microbial genomes. *Nucleic*
451 *Acids Res* 37(Database issue):D479–82.
- 452 10. Toledo-Arana A, et al. (2009) The *Listeria* transcriptional landscape from
453 saprophytism to virulence. *Nature* 459(7249):950–956.
- 454 11. Cho B-K, et al. (2009) The transcription unit architecture of the *Escherichia coli*
455 genome. *Nat Biotechnol* 27(11):1043–1049.

- 456 12. Güell M, et al. (2009) Transcriptome complexity in a genome-reduced bacterium.
457 *Science* 326(5957):1268–1271.
- 458 13. Wurtzel O, et al. (2010) A single-base resolution map of an archaeal
459 transcriptome. *Genome Res* 20(1):133–141.
- 460 14. Beaume M, et al. (2010) Cartography of Methicillin-Resistant *S. aureus*
461 Transcripts: Detection, Orientation and Temporal Expression during Growth
462 Phase and Stress Conditions. *PLoS ONE* 5(5):e10725.
- 463 15. Georg J, et al. (2009) Evidence for a major role of antisense RNAs in
464 cyanobacterial gene regulation. *Molecular Systems Biology* 5:305.
- 465 16. Dornenburg JE, DeVita AM, Palumbo MJ, Wade JT (2010) Widespread
466 Antisense Transcription in *Escherichia coli*. *mBio* 1(1):e00024–10–e00024–10.
- 467 17. Ruiz de Los Mozos I, et al. (2013) Base pairing interaction between 5'- and 3-
468 "UTRs controls *icaR* mRNA translation in *Staphylococcus aureus*. *PLoS*
469 *Genetics* 9(12):e1004001–e1004001.
- 470 18. Sesto N, Wurtzel O, Archambaud C, Sorek R, Cossart P (2013) The excludon: a
471 new concept in bacterial antisense RNA-mediated gene regulation. *Nat Rev*
472 *Micro* 11(2):75–82.
- 473 19. Thomason MK, Storz G (2010) Bacterial Antisense RNAs: How Many Are There,
474 and What Are They Doing? *Annu Rev Genet* 44(1):167–188.
- 475 20. Georg J, Hess WR (2011) *cis*-antisense RNA, another level of gene regulation in
476 bacteria. *Microbiol Mol Biol Rev* 75(2):286–300.
- 477 21. Lasa I, et al. (2011) Genome-wide antisense transcription drives mRNA
478 processing in bacteria. *Proc Natl Acad Sci U S A* 108(50):20172–20177.
- 479 22. Dean MA, Olsen RJ, Long SW, Rosato AE, Musser JM (2014) Identification of
480 point mutations in clinical *Staphylococcus aureus* strains that produce small-
481 colony variants auxotrophic for menadione. *Infect Immun* 82(4):1600–1605.
- 482 23. Mao F, Dam P, Chou J, Olman V, Xu Y (2009) DOOR: a database for
483 prokaryotic operons. *Nucleic Acids Res* 37(Database issue):D459–63.
- 484 24. Koch G, et al. (2014) Evolution of Resistance to a Last-Resort Antibiotic in
485 *Staphylococcus aureus* via Bacterial Competition. *Cell* 158(5):1060–1071.
- 486 25. Lioliou E, et al. (2012) Global Regulatory Functions of the *Staphylococcus*
487 *aureus* Endoribonuclease III in Gene Expression. *PLoS Genetics* 8(6):e1002782.
- 488 26. Lybecker M, Zimmermann B, Bilusic I, Tukhtubaeva N, Schroeder R (2014) The
489 double-stranded transcriptome of *Escherichia coli*. *Proc Natl Acad Sci U S A*
490 111(8):3134–3139.
- 491 27. Shearwin KE, Callen BP, Egan JB (2005) Transcriptional interference - a crash
492 course. *Trends Genet* 21(6):339–345.
- 493 28. Proctor RA, et al. (2006) Small colony variants: a pathogenic form of bacteria
494 that facilitates persistent and recurrent infections. *Nat Rev Micro* 4(4):295–305.

- 495 29. Sendi P, Proctor RA (2009) *Staphylococcus aureus* as an intracellular pathogen:
496 the role of small colony variants. *Trends in Microbiology* 17(2):54–58.
- 497 30. Brantl S (2007) Regulatory mechanisms employed by cis-encoded antisense
498 RNAs. *Curr Opin in Microbiol* 10(2):102–109.
- 499 31. Lasa I, Toledo-Arana A, Gingeras TR (2012) An effort to make sense of
500 antisense transcription in bacteria. *RNA biology* 9(8):1039–1044.
- 501 32. Opdyke JA, Fozo EM, Hemm MR, Storz G (2011) RNase III Participates in
502 GadY-Dependent Cleavage of the gadX-gadW mRNA. *Journal of Molecular*
503 *Biology* 406(1):29–43.
- 504 33. Krinke L, Wulff DL (1990) RNase III-dependent hydrolysis of lambda cII-O gene
505 mRNA mediated by lambda OOP antisense RNA. *Genes & Development*
506 4(12A):2223–2233.
- 507 34. Prescott EM, Proudfoot NJ (2002) Transcriptional collision between convergent
508 genes in budding yeast. *Proc Natl Acad Sci USA* 99(13):8796–8801.
- 509 35. Crampton N, Bonass WA, Kirkham J, Rivetti C, Thomson NH (2006) Collision
510 events between RNA polymerases in convergent transcription studied by atomic
511 force microscopy. *Nucleic Acids Res* 34(19):5416–5425.
- 512 36. Lloréns-Rico V, et al. (2016) Bacterial antisense RNAs are mainly the product of
513 transcriptional noise. *Sci Adv* 2(3):e1501363.
- 514 37. Proctor RA, et al. (2014) *Staphylococcus aureus* Small Colony Variants (SCVs):
515 a road map for the metabolic pathways involved in persistent infections. *Front*
516 *Cell Inf Microbio* 4(70):99.
- 517 38. Johns BE, Purdy KJ, Tucker NP, Maddocks SE (2015) Phenotypic and
518 genotypic characteristics of small colony variants and their role in chronic
519 Infection. *Microbiol Insights* 8:15–23.
- 520 39. Arnaud M, Chastanet A, Débarbouillé M (2004) New vector for efficient allelic
521 replacement in naturally nontransformable, low-GC-content, Gram-positive
522 bacteria. *Appl Environ Microbiol* 70(11):6887–6891.
- 523 40. Valle J, et al. (2003) SarA and not sigmaB is essential for biofilm development
524 by *Staphylococcus aureus*. *Mol Microbiol* 48(4):1075–1087.
- 525 41. King AN, et al. (2018) Guanine limitation results in CodY-dependent and -
526 independent alteration of *Staphylococcus aureus* physiology and gene
527 expression. *J Bacteriol.* doi:10.1128/JB.00136-18.
- 528 42. Poupel O, Proux C, Jagla B, Msadek T, Dubrac S (2018) SpdC, a novel
529 virulence factor, controls histidine kinase activity in *Staphylococcus aureus*.
530 *PLoS Pathog* 14(3):e1006917–32.
- 531 43. Bui LMG, Hoffmann P, Turnidge JD, Zilm PS, Kidd SP (2015) Prolonged growth
532 of a clinical *Staphylococcus aureus* strain selects for a stable small-colony-
533 variant cell type. *Infect Immun* 83(2):470–481.
- 534 44. Yeo W-S, et al. (2018) The FDA-approved anti-cancer drugs, streptozotocin and
535 floxuridine, reduce the virulence of *Staphylococcus aureus*. *Sci Rep* 8(1):2521.

536 **FIGURE LEGENDS**

537 **Figure 1. Analysis of the “non-contiguous operon” architecture.** JBrowse
538 software images showing RNA-seq or TSS-seq mapped reads distribution in the region
539 comprising *menE-menC-MW1733-ytkD-MW1731* genes of seven unrelated *S. aureus*
540 strains. The scale (\log_2 or $\times 10^3$) indicates the number of mapped reads per nucleotide
541 position. A schematic representation of the structure under study is shown in the
542 middle of the panel. ORFs are represented as orange arrows for the genes that
543 constitute the *menE-menC-ytkD-MW1731* operon and as a blue arrow for the *MW1733*
544 gene. Promoters are shown as green triangles and transcriptional terminators as red
545 rectangles. The transcript generated from the *menE-menC-ytkD-MW1731* operon is
546 represented as a dashed orange arrow whilst the transcript generated from *MW1733* is
547 presented as a dashed blue arrow. The top line denotes the position in base pairs of
548 the *S. aureus* MW2 genome. All genetic information about the start and the end of
549 transcription was obtained from a previous study (21). RNA seq data were obtained
550 from 15981 (21), MW2 (this study), UAMS-1 (41), HG001 (42), WCH-SK2 (43),
551 Homeland (24), USA300-P23 (44).

552

553 **Figure 2. Experimental evidence showing that the region comprising *menE-***
554 ***menC-MW1733-ytkD-MW1731* genes exhibits an architecture characteristic of a**
555 **non-contiguous operon.** (A) Western blots showing MenC, MW1731 or MW1733
556 protein levels in the wild-type (WT) and the following derivative strains: $\Delta Pmen$, *PblaZ-*
557 *men*, $\Delta PMW1733$ and *PblaZ-MW1733*. The 3xFLAG tagged proteins were detected
558 with commercial anti-3xFLAG antibodies. Coomassie stained or stain-free gel portions
559 are shown as a loading control. (B) Northern-blot analysis of RNA harvested from the
560 strains described in A. Blots were probed with specific riboprobes for *menEC*, *ytkD-*
561 *MW1731* and *MW1733* regions. The positions of RNA standards are indicated. Lower
562 panel shows 16S and 23S ribosome bands stained with ethidium bromide as loading
563 control. The strains used in this figure are depicted in Fig. S3.

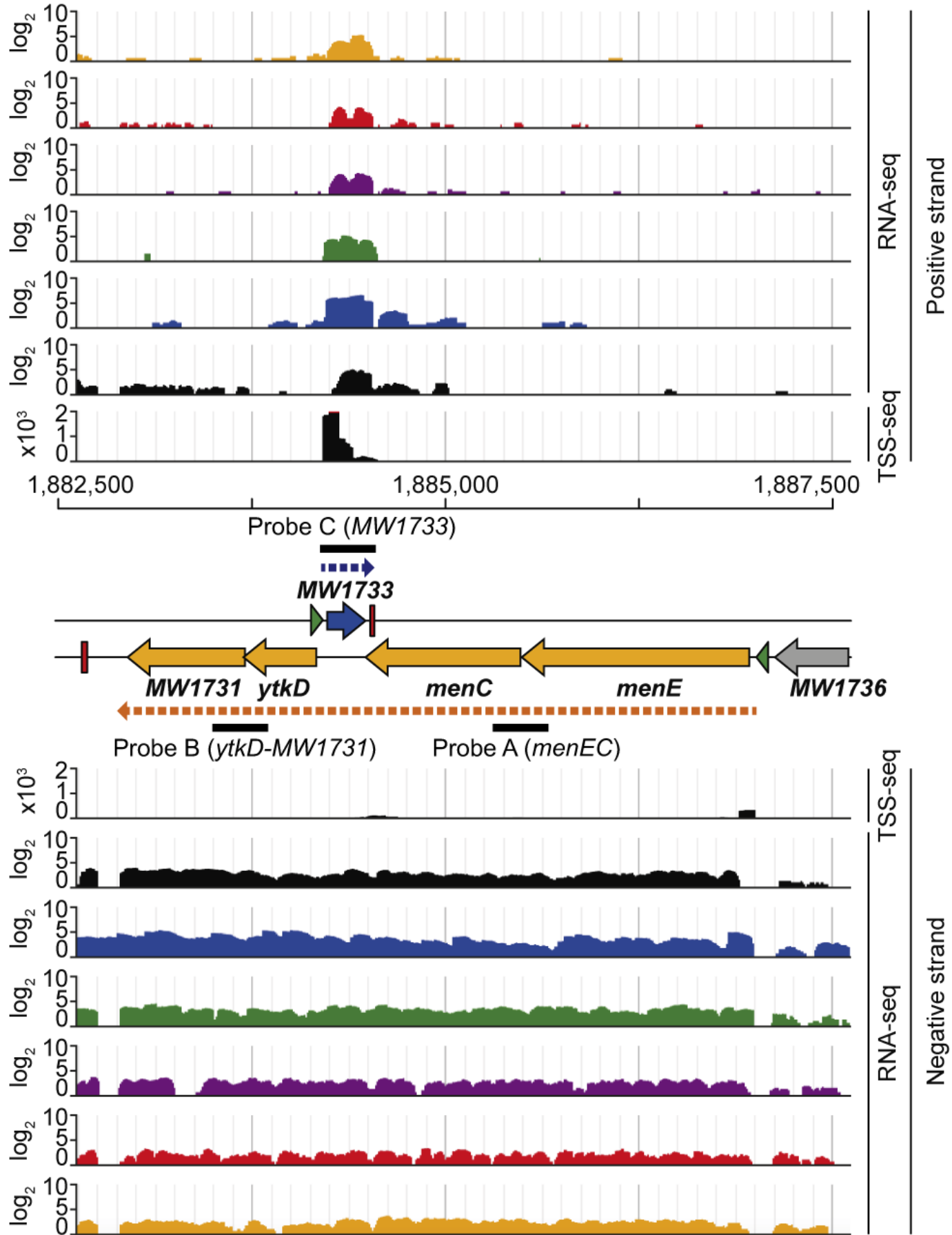
564

565 **Figure 3. Mutual regulation of overlapping transcripts expression within the non-**
566 **contiguous operon.** (A) Top: Northern blot showing *MW1733* mRNA levels in the WT,
567 $\Delta Pmen$ and *PblaZ-men* strains. A specific riboprobe (probe C) for *MW1733* was used;
568 Bottom: Western blot showing *MW1733* protein levels in the same strains producing a
569 3xFLAG tagged *MW1733* protein. (B) Top: Northern blot showing *menE-menC* mRNA
570 levels in the WT, $\Delta PMW1733$ and *PblaZ-MW1733* strains. A specific riboprobe (probe
571 A) for *menEC* was used; Bottom: Western blot showing MenC protein levels in the
572 same strains producing a 3xFLAG tagged MenC protein. (C) Top: Northern blot
573 showing *ytkD-MW1731* mRNA levels in the strains described in B. A specific riboprobe
574 (probe B) for *ytkD-MW1731* was used; Bottom: Western blot showing *MW1731* protein
575 levels in the same strains producing a 3xFLAG tagged *MW1731* protein. The positions
576 of RNA standards are indicated and 16S and 23S ribosome bands stained with ethidium
577 bromide are shown as loading controls. The 3xFLAG tagged proteins were detected
578 with commercial anti-3xFLAG antibodies. Coomassie stained or stain-free gel portions
579 are shown as a loading control. The strains used in this figure are depicted in Fig. S4.

580

581 **Figure 4. RNase III processing at the overlapping region and transcriptional**
582 **interference are involved in reciprocal regulation of the overlapping transcripts**
583 **generated from the non-contiguous operon.** (A) Top: Northern blot showing
584 *MW1733* mRNA levels in the WT, $\Delta PMW1733$, Δrnc , *PblaZ-men* and *PblaZ-men* Δrnc .
585 A specific riboprobe (probe C) for *MW1733* was used; Bottom: Western blot showing
586 *MW1733* protein levels in the same strains producing a 3xFLAG tagged *MW1733*
587 protein. (B) Top: Northern blot showing *menE-menC* mRNA levels in the WT, Δrnc ,
588 *PblaZ-MW1733* and *PblaZ-MW1733* Δrnc . A specific riboprobe (probe A) for *menE-*
589 *menC* was used; Bottom: Western blot showing MenC protein levels in the same
590 strains producing a 3xFLAG tagged MenC protein. (C) Top: Northern blot showing

591 *ytkD-MW1731* mRNA levels in the strains described in B. A specific riboprobe (probe
592 B) for *ytkD-MW1731* was used; Bottom: Western blot showing MW1731 protein levels
593 in the same strains producing a 3xFLAG tagged MW1731 protein. (D) Top: Northern
594 blot showing *MW1733* mRNA levels in the WT, *PblaZ-men*, Δ *PMW1733*, Δ *PMW1733*
595 *MW1733 trans* and Δ *PMW1733 PblaZ-men MW1733 trans*. A specific riboprobe (probe
596 C) for *MW1733* was used; Bottom: Western blot showing MW1733 protein levels in the
597 same strains producing a 3xFLAG tagged MW1733 protein. (E) Western blots showing
598 MenC (top) and MW1733 (bottom) protein levels in the WT, WT pCN40, *PblaZ-*
599 *MW1733* and WT pCN40::*MW1733-3xFLAG*. Strains contained a chromosomal copy of
600 either *menC* or *MW1731* tagged with the 3xFLAG epitope. The positions of RNA
601 standards are indicated and 16S and 23S ribosome bands stained with ethidium
602 bromide are shown as loading controls. The 3xFLAG tagged proteins were detected
603 with commercial anti-3xFLAG antibodies. Coomassie stained or stain-free gel portions
604 are shown as a loading control. The strains used in this figure are depicted in Fig. S5,
605 in the case of A, B, and C sections, and in Fig. S6 in the case of D and E sections.
606



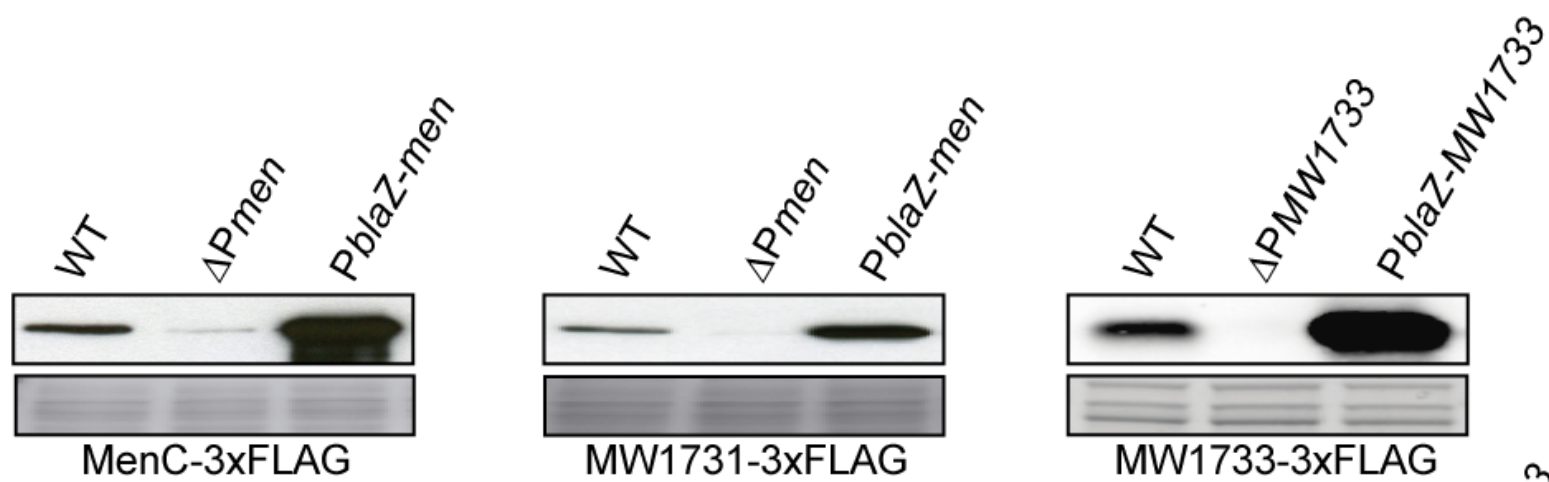
References

-----> Transcripts
 ➡ CDS
 ▶ Promoter
 ▬ Terminator

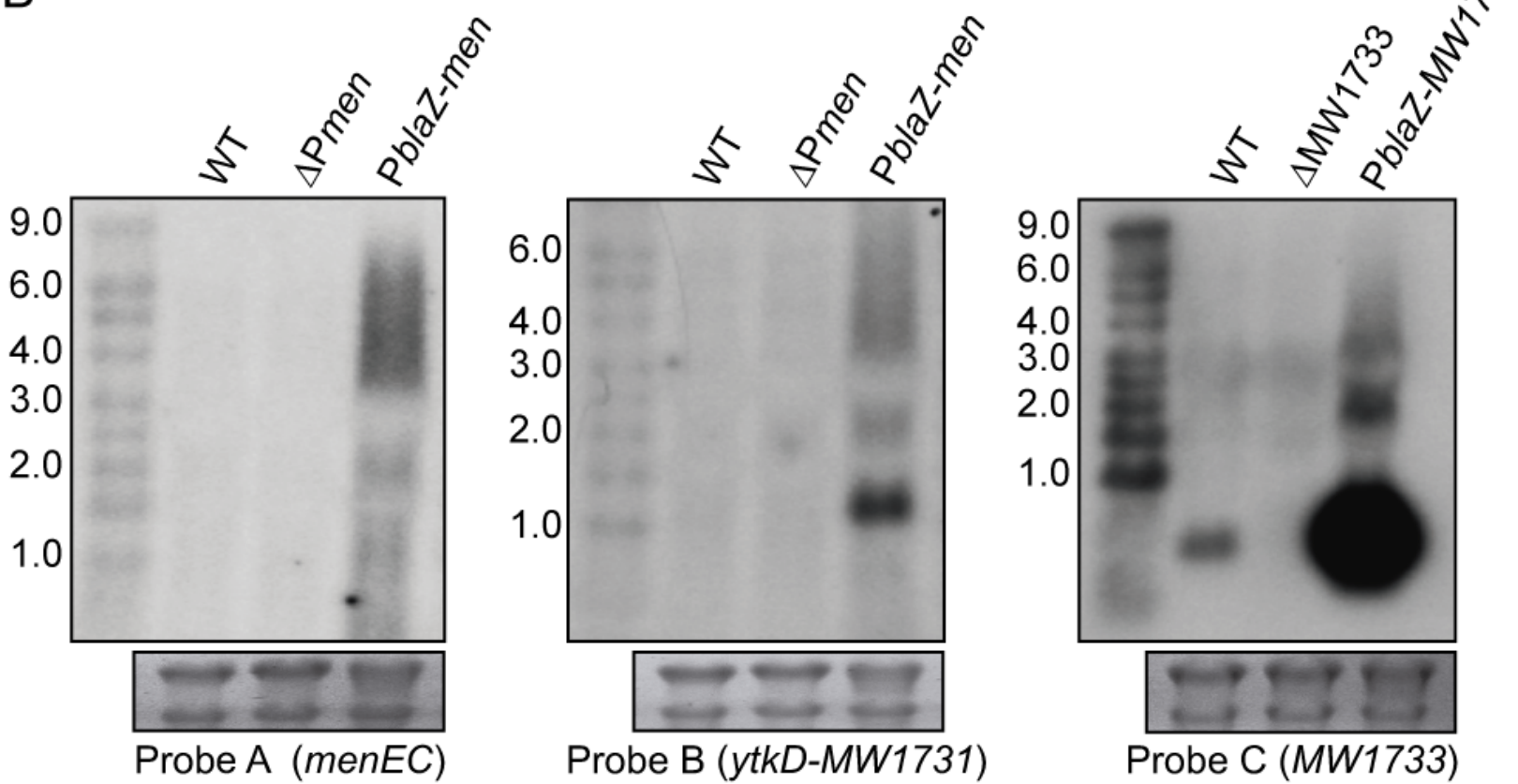
S. aureus strains

| RNA-seq | | | TSS-seq |
|--|--|--|---|
| ■ 15981 | ■ WCH-SK2 | ■ HG001 | ■ Homeland |
| ■ MW2 | ■ UAMS-1 | ■ USA300-P23 | |

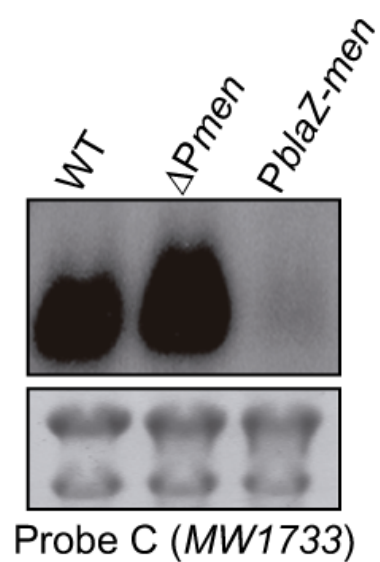
A



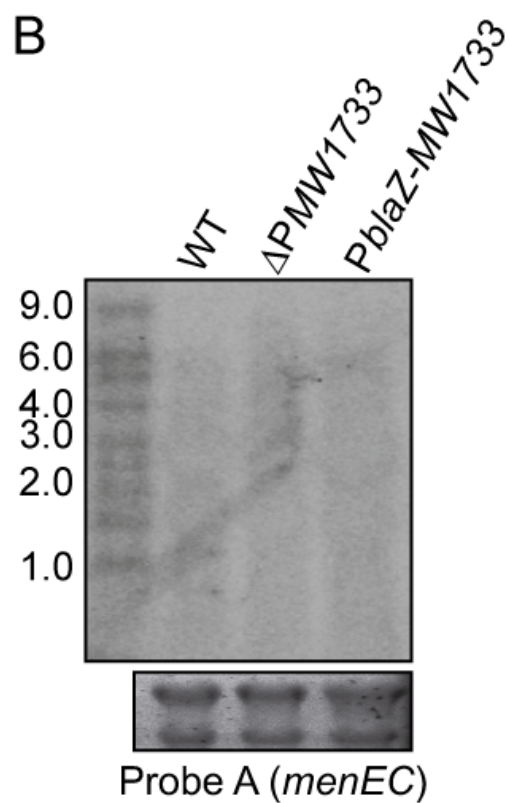
B



A



B



C

